

RSC Advances



This is an *Accepted Manuscript*, which has been through the Royal Society of Chemistry peer review process and has been accepted for publication.

Accepted Manuscripts are published online shortly after acceptance, before technical editing, formatting and proof reading. Using this free service, authors can make their results available to the community, in citable form, before we publish the edited article. This *Accepted Manuscript* will be replaced by the edited, formatted and paginated article as soon as this is available.

You can find more information about *Accepted Manuscripts* in the [Information for Authors](#).

Please note that technical editing may introduce minor changes to the text and/or graphics, which may alter content. The journal's standard [Terms & Conditions](#) and the [Ethical guidelines](#) still apply. In no event shall the Royal Society of Chemistry be held responsible for any errors or omissions in this *Accepted Manuscript* or any consequences arising from the use of any information it contains.

Cite this: DOI: 10.1039/c0xx00000x

www.rsc.org/xxxxxx

COMMUNICATION

A dual model logic gate for mercury and iodide ions sensing based on metal-organic framework MIL-101

Jing Mei Fang,^a Peng Fei Gao,^b Xiao Li Hu,^a Yuan Fang Li^{*a}

Received (in XXX, XXX) Xth XXXXXXXXX 20XX, Accepted Xth XXXXXXXXX 20XX

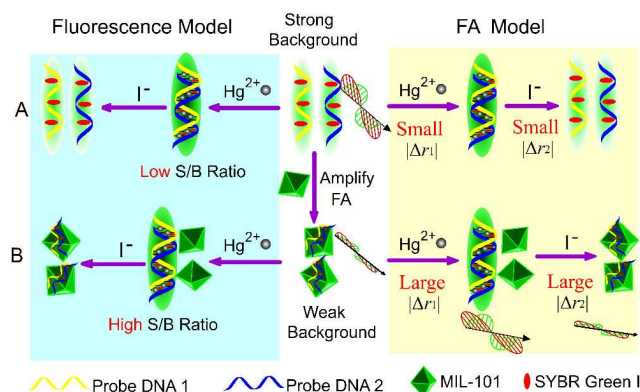
DOI: 10.1039/b000000x

Through the introduction of metal-organic framework MIL-101 as a low background signal and a fluorescence anisotropy amplification platform, a dual model DNA INHIBIT logic gate for Hg^{2+} and I^- detection has been designed.

Nowadays, DNA-based logic gates have attracted great interests because of the easy manipulation and multi-function of DNAs. They could be constructed based on the various behaviours of DNAs, including hybridization, cleavage and allosteric regulation *etc.*¹ The basic types of Boolean logic gates include AND, OR, NOT, INHIBIT, NOR, NAND, XOR, and XNOR.² Generally, in the field of analytical chemistry, the output signals of logic gates are colorimetry, fluorescence intensity or wavelength shift by the input of ions or small molecules.³ Fluorescence anisotropy (FA) is a spectroscopic technique that measures the rotational motion of a fluorescent molecule, which closely relates to the physical properties or local environments of the fluorophore. Therefore, FA is sensitive to the mass and size of the rotating body.⁴ As a high-throughput analysis assay, FA has been widely employed in the chiral molecular recognition^{4a} or the study of biomolecular interactions.⁵ For relatively small changes of the molecular weight in the reaction, the difference of FA is small, which is hard to measure. In order to overcome the difficulty, and with the development of nanotechnology, more and more materials have been employed as signal amplification platforms to increase the molecular weight, therefore generating a strong FA signal, including graphene oxide,⁶ golden nanoparticle,⁷ molecularly imprinted polymers (MIPs),⁸ protein⁹ *etc.* Also, FA is broadly used in the recognition of ions.¹⁰ However, introducing FA as the output signal of logic gates for ions detection has not been reported yet.

Some metal ions can bind with the nucleotide base specifically, such as cytosine- Ag^+ -cytosine (C- Ag^+ -C),¹¹ and thymine- Hg^{2+} -thymine (T- Hg^{2+} -T).¹² Up to now, a large number of DNA-based logic gates have been reported in the recognition of ions for its excellent selectivity, including ion-dependent DNazymes,¹³ aptamers,^{2a} and the methods coupled with graphene oxide¹⁴ as the quenchers *etc.* Metal-organic frameworks (MOFs) are a class of new porous nanomaterials, and have attracted tremendous attention in the field of analytical chemistry.¹⁵ For example, Yan *et al.* have employed MIL-53(Al) for highly selective and sensitive detection of Fe^{3+} in aqueous solution.¹⁶ According to our previous reports,¹⁷ MOF MIL-101

(chromium-benzenedicarboxylates, $\text{Cr}_3\text{F}(\text{H}_2\text{O})_2\text{O}[(\text{O}_2\text{C})-\text{C}_6\text{H}_4-(\text{CO}_2)]_3 \cdot n\text{H}_2\text{O}$) can be used as a low background platform for label-free DNA detection with the interacting-dye SYBR Green I (SG) as the fluorescence indicator. The results indicated that MIL-101 could distinguish the ssDNA and dsDNA effectively. Also, we have shown that MIL-101 was an efficiently FA amplification platform and successfully used in the detection of DNA.^{17b} So here we have introduced MIL-101 as a fluorescence quenching platform and FA amplification platform simultaneously. By this approach, a dual model logic gate for the detection of mercury and iodide ions could be constructed, and it is the first time that introducing the FA as output signal of logic gate.



Scheme 1 Schematic illustration for the detection of Hg^{2+} and I^- . (A) Without MIL-101, high background signal, and the change of FA is small; (B) with MIL-101, the background signal is low, and the change of FA is large.

In this contribution, based on MIL-101, we employed SG as the indicator, and two separate T-rich ssDNA (P1: 5'-TTC TTT CAT TTC TTT CTT CG-3', P2: 5'-CG TTG TTT GTT ATG TTT GTT-3') as probe oligonucleotides to design a dual model logic gate. In the absence of MIL-101, the signal-to-background ratio is relatively lower owing to the high background fluorescence of SG/P; the deviation for both the mass and the size of SG between the single-stranded and the double-stranded are restricted, so the value change of FA is too small to measure (scheme 1A). However, as shown in scheme 1B, the signal-to-background ratio and the value change of FA are both increased through the introduction of MIL-101. The flexible SG/P complex can be adsorbed on the surface of MIL-101 by means of π - π stacking and electrostatic interactions between nucleotide bases and

MIL-101,^{17a} thus the fluorescence of SG/P can be quenched. As a consequence, the background signal is lower. Meanwhile, as SG/P is adsorbed on MIL-101, the mass and size of SG is enlarged, the rotation of SG is restricted, then resulting in the enhancement of the FA signal. When Hg²⁺ is present, Hg²⁺ can bind between the N3 of the thymine,^{12a} the T-T mismatched base can form T-Hg²⁺-T base pairs. Thus, the fluorescence of SG is enhanced as it binds with the dsDNA in the mode of intercalation and minor groove binding.¹⁸ Since the dsDNA can be far away from the surface of MIL-101, the rotation of SG is relatively free, leading to a decreasing of the FA value.^{17a} Thus, Hg²⁺ can be detected by the large value change of FA. As is well-known, Γ ion is a strong Hg²⁺-binder, and can be used to unfold the T-Hg²⁺-T double-stranded structure. Therefore, in the presence of Γ , the SG/P can be adsorbed on MIL-101 again. Consequently, the fluorescence of SG is decreased, and the FA of SG is enhanced. As expected, a new detection method of Hg²⁺ and Γ has been successfully constructed. Simultaneously, a new MIL-101 based Hg²⁺/ Γ -driven fluorescence intensity and fluorescence anisotropy dual model DNA INHIBIT logic gate has also been designed.

In order to quantify Hg²⁺ and Γ better, several factors, such as the reaction time for hybridization and fluorescence quenching (Fig. S1), pH value (Fig. S2), and the dosage of MIL-101 (Fig. S3) were optimized. The high background signal of SG/P decreased significantly on employing MIL-101, thus increasing the signal-to-background ratio (expressed as F/F_0 , where F and F_0 represent the fluorescence intensity of SG in the presence or absence of Hg²⁺, respectively) as high as ~5-fold (Fig. S4). In the FA experiments, with the introduction of MIL-101, the value change of FA in the absence or presence of the target (expressed as $|\Delta r_1|$) have improved ~45-fold and ~23-fold for the Hg²⁺ and Γ , respectively (Fig. S5). All the results showed that MIL-101 was not only an efficiently low background platform but also an FA amplification platform.

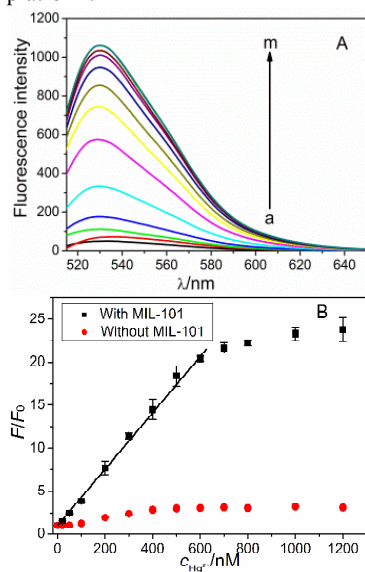


Fig. 1 (A) Fluorescence emission spectra of SG/P/MIL-101 upon the addition of Hg²⁺. (B) The signal-to-background ratio (F/F_0) histogram of SG/P/MIL-101 (squares) and SG/P (diamonds) with increasing concentration of Hg²⁺. Concentrations: Hg²⁺, a \rightarrow m, 0, 20, 50, 100, 200, 300, 400, 500, 600, 700, 800, 1000, 1200 nM; SG, 0.245 μ M; P1, 20 nM; P2, 20 nM; MIL-101, 36 μ g-mL⁻¹. Tris-HCl buffer, pH 7.6.

To test the sensitivity for Hg²⁺ detection, the system was mixed with various amounts of Hg²⁺ under the optimal conditions. As shown in Fig. 1A, with the increasing concentration of Hg²⁺, the fluorescence intensity of SG/P/MIL-101 increases gradually. Fig. 1B shows the F/F_0 plotted against the concentration of Hg²⁺, indicating that the F/F_0 in the presence of MIL-101 is much higher than that in the absence of MIL-101, and the linear range is from 20 to 600 nM with the equation $F/F_0=0.033c_{\text{Hg}^{2+}}$ (nM)+0.68, $R=0.998$ (Fig. 1B). It confirmed that the detection limit was as low as 10.5 nM (based on $3\sigma/\text{slope}$). In the FA method, with the addition of Hg²⁺, the FA of SG/P/MIL-101 decreased gradually. The value change of FA was expressed as $|\Delta r_1|$ ($|\Delta r_1|=|r_1-r_2|$, wherein r_1 and r_2 stand for the FA values of the SG/P/MIL-101 in the absence and presence of Hg²⁺, respectively). As shown in Fig. 2A, the linear range is from 20 to 200 nM with the equation $|\Delta r_1|=0.036+7.08\times 10^{-4}c_{\text{Hg}^{2+}}$ (nM), $R=0.993$, and the detection limit is 8.66 nM.

To validate the selectivity of this assay for Hg²⁺ detection, competing metal ions, including Al³⁺, Fe³⁺, Cr³⁺, Ni²⁺, Co²⁺, Cu²⁺, Zn²⁺, Mg²⁺, Ba²⁺, Ca²⁺ and K⁺ were tested under the same conditions with a concentration 5 times higher than that of Hg²⁺. The results showed that both the F/F_0 and the $|\Delta r_1|$ of the system had little change in the presence of the majority of the interfering metal ions (Fig. S6), indicating the designed method had excellent selectivity for the Hg²⁺ detection over other metal ions.

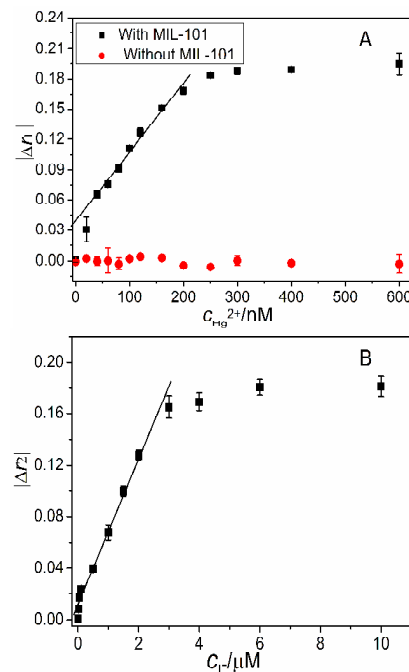


Fig. 2 (A) The changes of $|\Delta r_1|$ with different concentration of Hg²⁺: 0, 20, 40, 60, 80, 100, 120, 160, 200, 250, 300, 400, 600 nM. (B) The changes of $|\Delta r_2|$ with different concentration of Γ : 0, 0.02, 0.05, 0.1, 0.5, 1.0, 1.5, 2.0, 3.0, 4.0, 6.0, 10 μ M; Hg²⁺, 200 nM. Concentrations: SG, 0.245 μ M; P1, 20 nM; P2, 20 nM; MIL-101, 33 μ g-mL⁻¹. Tris-HCl buffer, pH 7.6.

As discussed previously, Γ as a second input will change the fluorescence intensity and FA of the system. As shown in Fig. 3A, with the increasing concentration of Γ , a gradual decrease of the fluorescence intensity is observed, indicating the competition between Γ and thymine for Hg²⁺. Fig. 3B shows the F/F_0 plotted against the concentration of Γ , and the linear range is from 0.05

to 1.6 μM with the equation $F/F_0=85-35c_{\Gamma}$ (nM), $R=0.994$ (Fig. 3B), the detection limit is 13 nM. In the FA method, the FA of SG/P/Hg²⁺/MIL-101 was increased gradually with the addition of Γ , and the value change of FA was expressed as $|\Delta r_2|$ ($|\Delta r_2|=|r_2-r_3|$, wherein r_2 and r_3 stand for the FA values of the SG/P/Hg²⁺/MIL-101 in the absence and presence of Γ , respectively). As shown in Fig. 2B, the linear range is from 0.02 to 3.0 μM with the equation $|\Delta r_2|=0.014+0.055c_{\Gamma}$ (μM), $R=0.990$, and the detection limit is 17.4 nM.

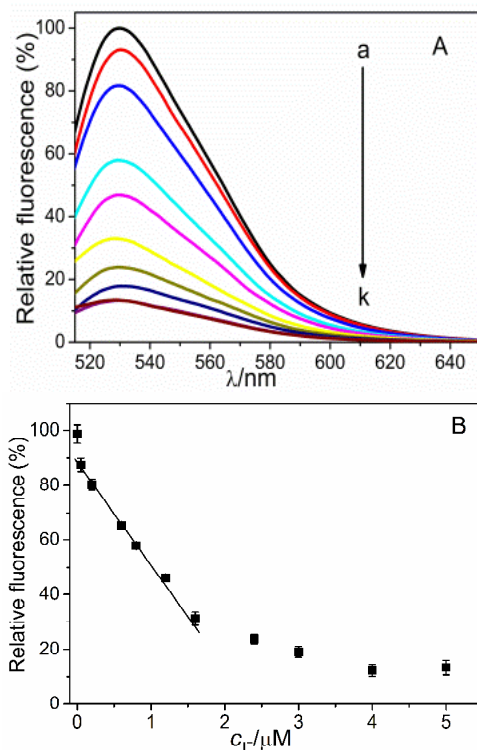


Fig. 3 (A) Fluorescence emission spectra of SG/P/Hg²⁺/MIL-101 upon the addition of Γ . (B) The changes of fluorescence intensity at 529 nm with different concentration of Γ . Concentrations: Hg²⁺, 500 nM; Γ , a \rightarrow k, 0, 0.05, 0.1, 0.2, 0.4, 0.8, 1.6, 2.4, 3.0, 4.0, 5.0 μM ; SG, 0.245 μM ; P1, 20 nM; P2, 20 nM; MIL-101, 36 $\mu\text{g}\cdot\text{mL}^{-1}$. Tris-HCl buffer, pH 7.6.

The selectivity of this assay for the detection of Γ was investigated by testing common competing anions, including F^- , Cl^- , Br^- , BrO_3^- , IO_3^- , SO_4^{2-} , HCO_3^- , NO_3^- , HPO_4^{2-} and SCN^- , which undergoes the same conditions with a concentration 5 times higher than that of Γ . For the fluorescence method, the results showed that only Γ decreased the fluorescence intensity dramatically, showing an 86.1% decrease of the original value (Fig. S7A). For the FA method, only Γ caused a large change of $|\Delta r_2|$ (Fig. S7B), while other anions showed insignificant changes to the detection signals of the SG/P/Hg²⁺/MIL-101 system. Overall, the sensitivity and selectivity investigation for Γ detection demonstrated that the SG/P/Hg²⁺/MIL-101 system is suitable for the detection of Γ over other competing anions in both fluorescence and FA methods.

The Hg²⁺/ Γ mediated fluorescence intensity and FA changes in the sensing system enable a dual model DNA INHIBIT logic gate. Here, Hg²⁺ and Γ are defined as the two inputs for the logic gate; fluorescence and FA signals are defined as the two outputs. The four possible input combinations are shown in the truth table

(Fig. 4D), including (0, 0), (0, 1), (1, 0) and (1, 1). For input, the presence of Hg²⁺ or Γ is defined as 1 and the absence as 0. In the absence of both Hg²⁺ and Γ (0, 0), the fluorescence intensity of the system is weak, the FA signal is strong, and we define the outputs as 0, respectively. While only in the presence of Γ (0, 1), the outputs are both still 0. In the presence of Hg²⁺ (1, 0), the fluorescence intensity of the system is strong, the FA signal is weak, and we define the outputs as 1, respectively. When in the presence of both Hg²⁺ and Γ (1, 1), the outputs are also 0. Therefore, in the whole progress, only the introduction of Hg²⁺ can lead to the dramatic change of the output signal (Fig. 4A, B, C); meanwhile, Fig. 4B (light grey) showed that the value changes of FA are very small in the absence of MIL-101, and it could not be used for the detection of Hg²⁺ and Γ . This is a new concept for performance of DNA logic gate and it is the first example of a MIL-101-based Hg²⁺/ Γ -driven dual model DNA INHIBIT logic gate. Our study provides a new strategy with potential applications in monitoring Hg²⁺ and Γ in environmental samples. The determination results of Hg²⁺ and Γ with the two methods in tap water are given in Table S1.

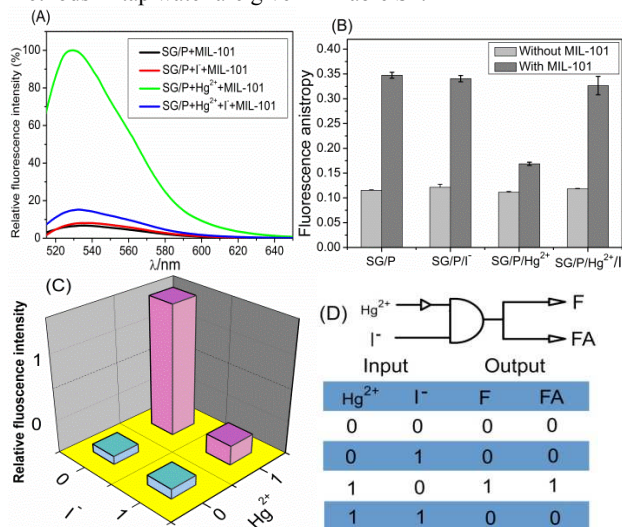


Fig. 4 (A) Fluorescence emission spectra of SG/P in different conditions, Hg²⁺, 500 nM; Γ , 3 μM ; MIL-101, 36 $\mu\text{g}\cdot\text{mL}^{-1}$. (B) The FA of SG/P in the presence of 200 nM Hg²⁺, 3.0 μM Γ and 33 $\mu\text{g}\cdot\text{mL}^{-1}$ MIL-101, respectively. (C) Fluorescence intensity at 529 nm in the form of a bar representation. (D) Truth table for the two-input and two-output INHIBIT logic gate. Concentrations: SG, 0.245 μM ; P1, 20 nM; P2, 20 nM. Tris-HCl buffer, pH 7.6.

In conclusion, we have employed MIL-101 as both the low background signal and FA amplification platform to construct a dual model logic gate for the detection of Hg²⁺ and Γ . The proposed method presents several advantages: a) it is label-free; b) comparing to the reported methods,^{2a, 14} it has high sensitivity for the determination of Γ . For the detection of Hg²⁺, the sensitivity is comparable to that reported in the literatures;¹⁹ c) it is the first time that introducing FA as output signal of logic gate, expanding the application of FA and MOFs.

The authors are grateful for financial support from the National Natural Science Foundation of China (NSFC, No. 21175109) and the special fund of Chongqing key laboratory (CSTC).

Notes and references

^aKey Laboratory of Luminescent and Real-Time Analytical Chemistry (Southwest University), Ministry of Education, College of Chemistry and Chemical Engineering, Southwest University, Chongqing, 400715, PR China. Fax: (+86) 23 68367257; Tel: (+86) 23 68254659; E-mail:

⁵ liyjf@swu.edu.cn

^bCollege of Pharmaceutical Sciences, Southwest University, Chongqing, 400715, PR China.

† Electronic Supplementary Information (ESI) available: [details of any supplementary information available should be included here]. See

DOI: 10.1039/b000000x/

1. K. Sakamoto, H. Gouzu, K. Komiya, D. Kiga, S. Yokoyama, T. Yokomori and M. Hagiya, *Science*, 2000, **288**, 1223.
2. (a)X. Wu, J. Chen and J. X. Zhao, *Analyst*, 2013, **138**, 5281; (b)A. P. d. Silva and N. D. McClenaghan, *Chem. Eur. J.*, 2004, **10**, 574; (c)E. Katz, *Molecular and Supramolecular Information Processing: From Molecular Switches to Logic Systems*, Wiley, 2012.
- 15 3. (a)J. Ren, J. Wang and E. Wang, *Chem. Eur. J.*, 2013, **19**, 479; (b)W. Y. Xie, W. T. Huang, N. B. Li and H. Q. Luo, *Chem. Commun.*, 2012, **48**, 82; (c)T. Gunnlaugsson, D. A. M. Dónaila and D. Parkerb, *Chem. Commun.*, 2000, 93; (d)T. Li, E. Wang and S. Dong, *J. Am. Chem. Soc.*, 2009, **131**, 15082.
4. (a)M. E. McCarroll, F. H. Billiot and I. M. Warner, *J. Am. Chem. Soc.*, 2001, **123**, 3173; (b)A. B. Rawitch and G. Weber, *J. Biol. Chem.*, 1972, **247**, 680.
- 25 5. (a)D. M. Jameson and W. H. Sawyer, *Method. Enzymol.*, 1995, **246**, 283; (b)T. Heyduk, Y. Ma, H. Tang and R. H. Ebright, *Method. Enzymol.*, 1996, **274**, 492; (c)Y. Yan and G. Marriott, *Curr. Opin. Chem. Biol.*, 2003, **7**, 635.
6. (a)J. Liu, C. Wang, Y. Jiang, Y. Hu, J. Li, S. Yang, Y. Li, R. Yang, W. Tan and C. Z. Huang, *Anal. Chem.*, 2013, **85**, 1424; (b)Y. Yu, Y. Liu, S. J. Zhen and C. Z. Huang, *Chem. Commun.*, 2013, **49**, 1942.
- 30 7. (a)X. Wang, M. Zou, H. Huang, Y. Ren, L. Li, X. Yang and N. Li, *Biosens. Bioelectron.*, 2013, **41**, 569; (b)Y. Huang, J. Chen, M. Shi, S. Zhao, Z.-F. Chen and H. Liang, *J. Mater. Chem. B*, 2013, **1**, 2018.
- 35 8. C. E. Hunt, P. Pasetto, R. J. Ansell and K. Haupt, *Chem. Commun.*, 2006, 1754.
9. (a)J. Zhang, J. Tian, Y. He, S. Chen, Y. Jiang, Y. Zhao and S. Zhao, *Analyst*, 2013, **138**, 4722; (b)Z. Zhu, C. Ravelet, S. Perrier, V. Guieu, E. Fiore and E. Peyrin, *Anal. Chem.*, 2012, **84**, 7203; (c)M. Zou, Y. Chen, X. Xu, H. Huang, F. Liu and N. Li, *Biosens. Bioelectron.*, 2012, **32**, 148.
- 40 10. (a)B. C. Ye and B. C. Yin, *Angew. Chem. Int. Ed.*, 2008, **47**, 8386; (b)J. Zhang, J. Tian, Y. He, Y. Zhao and S. Zhao, *Chem. Commun.*, 2014, **50**, 2049.
- 45 11. (a)A. Ono, S. Cao, H. Togashi, M. Tashiro, T. Fujimoto, T. Machinami, S. Oda, Y. Miyake, I. Okamoto and Y. Tanaka, *Chem. Commun.*, 2008, 4825; (b)L. Liu, D. Zhang, G. Zhang, J. Xiang and D. Zhu, *Org. Lett.*, 2008, **10**, 2271.
12. (a)Y. Miyake, H. Togashi, M. Tashiro, H. Yamaguchi, S. Oda, M. Kudo, Y. Tanaka, Y. Kondo, R. Sawa, T. Fujimoto, T. Machinami and A. Ono, *J. Am. Chem. Soc.*, 2006, **128**, 2172; (b)L. Liu, G. Zhang, J. Xiang, D. Zhang and D. Zhu, *Org. Lett.*, 2008, **10**, 4581.
- 50 13. L. Zhang, Y. M. Zhang, R. P. Liang and J. D. Qiu, *J. Phys. Chem. C*, 2013, **117**, 12352.
- 55 14. M. Zhang and B. C. Ye, *Chem. Commun.*, 2012, **48**, 3647.
15. (a)Z. Y. Gu, C. X. Yang, N. Chang and X. P. Yan, *Accounts Chem. Res.*, 2012, **45**, 734; (b)Y. L. Liu, X. J. Zhao, X. X. Yang and Y. F. Li, *Analyst*, 2013, **138**, 4526; (c)X. J. Zhao, R. X. He and Y. F. Li, *Analyst*, 2012, **137**, 5190; (d)X. Zhu, H. Y. Zheng, X. F. Wei, Z. Y. Lin, L. H. Guo, B. Qiu and G. N. Chen, *Chem. Commun.*, 2013, **49**, 1276; (e)X. J. Zhao, J. H. Yang, Y. Liu, P. F. Gao and Y. F. Li, *RSC Advances*, 2014, **4**, 2573.
16. C. X. Yang, H. B. Ren and X. P. Yan, *Anal. Chem.*, 2013, **85**, 7441.
17. (a)J. M. Fang, F. Leng, X. J. Zhao, X. L. Hu and Y. F. Li, *Analyst*, 2014, **139**, 801; (b)J. F. Guo, C. M. Li, X. L. Hu, C. Z. Huang and Y. F. Li, *RSC Advances*, 2014, **4**, 9379.
- 65 18. H. Zipper, H. Brunner, J. Bernhagen and F. Vitzthum, *Nucleic Acids Res.*, 2004, **32**, e103.
19. (a)A. P. Fan, Y. Ling, C. Lau and J. Z. Lu, *Talanta* 2010, **82**, 687; (b)M. Zhang and B. C. Ye, *Chem. Commun.*, 2012, **48**, 3647.
- 70